The EMBO Journal Vol.18 No.14 pp.4076–4084, 1999

Mechanism of DNA segregation in prokaryotes: ParM partitioning protein of plasmid R1 co-localizes with its replicon during the cell cycle

Rasmus Bugge Jensen[1] and Kenn Gerdes[2]

Department of Molecular Biology, Odense University, Campusvej 55, DK-5230 Odense M, Denmark

[1]Present address: Department of Developmental Biology, Stanford University School of Medicine, Stanford, CA 94305-5329, USA

[2]Corresponding author
e-mail: kgerdes@molbiol.ou.dk

The *parA* locus of plasmid R1 encodes a prokaryotic centromere-like system that mediates genetic stabilization of plasmids by an unknown mechanism. The locus codes for two proteins, ParM and ParR, and a centromere-like DNA region (*parC*) to which the ParR protein binds. We showed recently that ParR mediates specific pairing of *parC*-containing DNA molecules *in vitro*. To obtain further insight into the mechanism of plasmid stabilization, we examined the intracellular localization of the components of the *parA* system. We found that ParM forms discrete foci that localize to specific cellular regions in a simple, yet dynamic pattern. In newborn cells, ParM foci were present close to both cell poles. Concomitant with cell growth, new foci formed at mid-cell. A point mutation that abolished the ATPase activity of ParM simultaneously prevented cellular localization and plasmid partitioning. A *parA*-containing plasmid localized to similar sites, i.e. close to the poles and at mid-cell, thus indicating that the plasmid co-localizes with ParM. Double labelling of single cells showed that plasmid DNA and ParM indeed co-localize. Thus, our data indicate that *parA* is a true partitioning system that mediates pairing of plasmids at mid-cell and subsequently moves them to the cell poles before cell division.

Keywords: GFP/intracellular localization/*parA*/partitioning/plasmid segregation

Introduction

Accurate distribution of genetic material to progeny cells at cell division is essential for all organisms. Despite the central role of DNA segregation in the bacterial cell cycle, the molecular mechanism of the process is not well understood. Model plasmids, such as R1, F and P1, contain several different types of systems that prevent plasmid loss at cell division (reviewed by Nordström and Austin, 1989; Hiraga, 1992). One such type encodes a differentiation programme that leads to killing of plasmid-free cells and thereby confers plasmid stabilization (reviewed by Jensen and Gerdes, 1995; Gerdes *et al.*, 1997). In contrast, true partitioning systems stabilize their replicons by actively distributing the plasmid molecules. In molecular terms, plasmid-encoded *par* genes are the best characterized determinants of DNA segregation in bacteria. Bacterial chromosomes contain genes that are homologous to the *par* genes from plasmids. In *Bacillus subtilis* (*soj* and *spo0J*) and *Caulobacter crescentus* (*parA* and *parB*), such genes are known to be involved in chromosome segregation (Ireton *et al.*, 1994; Sharpe and Errington, 1996; Mohl and Gober, 1997). The recent molecular genetic and cytological analyses of the DNA segregation process in prokaryotes has demonstrated that the *par* genes specify centromere-like systems that pair and separate DNA molecules in an ordered sequence (Harry, 1997; Wheeler and Shapiro, 1997; Jensen *et al*., 1998; Sharpe and Errington, 1999).

In general, plasmid partitioning systems are composed of a *cis*-acting centromere-like site and two genes that encode proteins required for the partitioning process. In the *parA* system of plasmid R1, the *cis*-acting *parC* site is located upstream of the genes encoding ParM (motor protein) and ParR (repressor) (see Figure 1; Gerdes and Molin, 1986; Dam and Gerdes, 1994). The 160 bp *parC* site contains the *parA* promoter flanked by two sets of five direct repeats (iterons) to which the ParR protein binds (Jensen *et al*., 1994, 1998; Breüner *et al.*, 1996). The presence of all 10 iterons is required for plasmid partitioning and for regulation of the *parA* promoter (Dam and Gerdes, 1994; Jensen *et al.*, 1994; Breüner *et al.*, 1996). The ParM protein has ATPase activity that is stimulated by ParR when ParR is bound to *parC* (Jensen and Gerdes, 1997). Single amino acid changes in ParM that inactivate the ATPase activity also abolish *in vivo* partitioning. Recently, we showed that the *parA* system mediates efficient pairing of plasmid molecules *in vitro* (Jensen *et al.*, 1998). Pairing required the presence of *parC* bound by ParR. The pairing reaction was stimulated further by supercoiling and by ParM in the presence of ATP. This suggested that replicon pairing is an essential step in the partitioning process (Jensen *et al*., 1998). Thus post-replicational pairing of DNA molecules occurs in prokaryotes as well as in eukaryotes.

The second family of prokaryotic partitioning systems includes *par* of P1 and *sop* of F (Ogura and Hiraga, 1983; Abeles *et al.*, 1985). In the P1 *par* and F *sop* systems, the centromere-like sites *parS* and *sopC* are located downstream of the genes encoding the partitioning proteins (Ogura and Hiraga, 1983; Abeles *et al.*, 1985). ATPase activity and DNA-binding activities have also been described for the partitioning proteins of P1 and F (Davis and Austin, 1988; Mori *et al.*, 1989; Davis *et al.*, 1992; Watanabe *et al.*, 1992). The P1 and F plasmids and the SopB partitioning protein are positioned at mid-cell or at 1/4 and 3/4 positions (Gordon *et al.*, 1997; Niki and Hiraga, 1997; Kim and Wang, 1998).

The *parA* system of plasmid R1 shows no sequence similarity at the protein or nucleic acid levels to the

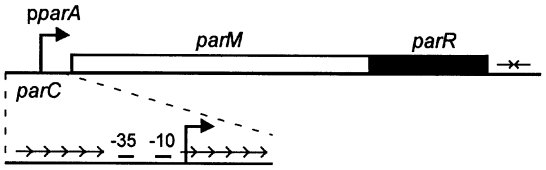

Fig. 1. Overview of the *parA* partitioning system of plasmid R1 with an enlargement of the *parC* region. The *parM* gene is shown as an open bar and the *parR* gene as a black bar. The 10 direct repeats (iterons) in *parC* are shown as arrows, the –35 and –10 sequences of the *parA* promoter are marked with lines, and the transcriptional start point is shown as an arrow pointing to the right. The transcriptional terminator of the operon is shown as opposing arrows.

systems of the *par/sop* family. Elucidation of the molecular mechanism of plasmid partitioning by *parA* may therefore provide new insights into the process of DNA segregation. Here we examine the intracellular localization of the ParM and ParR proteins using fusions to green fluorescent protein (GFP) and immunofluorescence microscopy (IFM). We also use a GFP–LacI fusion protein to visualize the intracellular position of a plasmid partitioned by the *parA* system. Fluorescence and phase-contrast microscopy reveal that the ParM protein and the *parA*-containing plasmid co-localize at specific sites near the cell poles or at mid-cell. These results demonstrate that *parA* of R1 specifies a true partitioning system and suggest a process that involves pairing of newly replicated plasmids at mid-cell followed by separation, and active movement to the poles of the pre-divisional cell.

Results

Properties of ParM–GFP fusion proteins

To study the subcellular localization of ParM, we constructed gene fusions to a bright variant (Mut1) of GFP from *Aequorea victoria* (Cormack *et al.*, 1996). Full-length ParM was fused to both the N- (ParM–GFP) and the C-terminus of GFP (GFP–ParM) (Figure 2A). Protein fusions were also made to truncated or mutated ParM. The GFP fusion proteins were expressed from the *lac* promoter, rendering expression inducible by isopropyl-β-D-thiogalactopyranoside (IPTG). Using Western analysis, we confirmed that all fusion proteins were expressed and had the expected sizes (data not shown). With the induction conditions used here (see Materials and methods), the amount of ParM–GFP fusion protein in the cell was close to the amount of ParM expressed from a wild-type *parA* system resident in R1 (1.5- to 2.5-fold overproduction).

We then tested the functionality of the fusion proteins. The mini-R1 test plasmid pDD1509K, that contains a *parA* system with a deletion in *parM*, was not stabilized when the fusion proteins were expressed *in trans* from a co-resident plasmid. However, expression of ParM–GFP destabilized the $parA^+$ mini-R1 test-plasmid pAB1503 500-fold, corresponding to active destabilization. Thus, ParM–GFP exhibits *trans*-dominance since it overrides wild-type ParM.

Visualization of the subcellular localization of ParM using GFP fusion proteins

The subcellular localization of fusions between ParM and GFP was examined using combined fluorescence and phase-contrast microscopy. Figure 3A shows cells

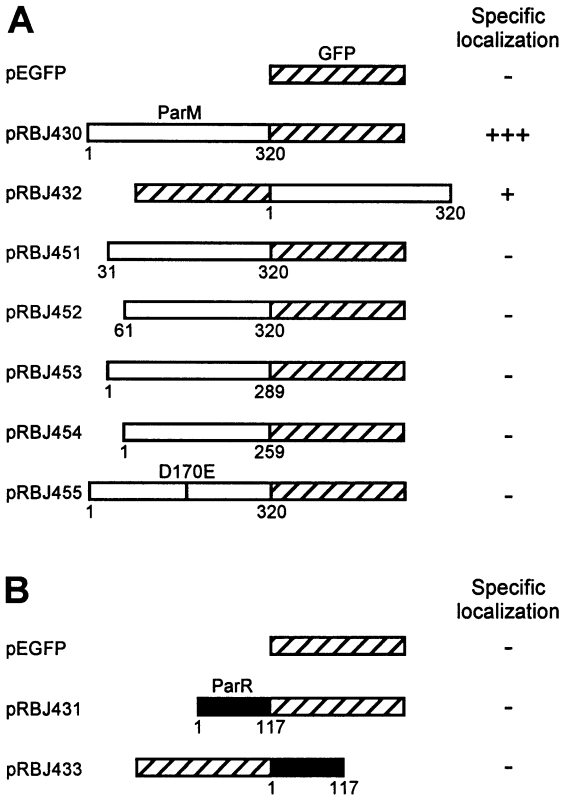

Fig. 2. ParM, ParR and GFP fusion proteins used in this work. (**A**) Full-length or truncated ParM fused to GFP. (**B**) Full-length ParR fused to GFP. ParM is symbolized as open boxes, ParR as black boxes and GFP as hatched boxes. The numbers indicate the amino acid residues of ParM or ParR that are present in the fusion proteins. The vertical bar shows the location of the D170E mutation in ParM. This mutation reduces the ATPase activity of ParM (Jensen and Gerdes, 1997). The degree of localization as determined using fluorescence microscopy is indicated in the right column. Minus indicates no specific localization and plus indicates the observation of localization of the GFP fusion protein to specific sites.

expressing the ParM–GFP protein. No other components of the R1 *parA* system were present. The majority of the cells (80–90%) showed localization of ParM–GFP to specific positions in the cell. Three different types of cells were observed (Figure 3B). Small cells contained two GFP foci specifically located to regions close to but not at the cell poles (Figure 3A, a–c). Larger cells contained three GFP foci; two foci were located close to the cell poles, and the third focus was located at mid-cell (Figure 3A, d–f). Pre-divisional cells contained four GFP foci, two of which were located close to the cell poles and two close to mid-cell (Figure 3A, g–j). In some cells, the two mid-cell foci were located very close to each other (Figure 3A, g and h) and in others the mid-cell foci were more separated (Figure 3A, i and j). The ParM–GFP foci were found to be located symmetrically in the vast majority of the cells (all of the 340 cells examined). The positions of the ParM–GFP foci relative to the cell poles were measured for cells of all types and different lengths. The polar foci were found to be located at a fixed distance from the cell pole that was independent of the cell length. The distribution of the ParM–GFP foci as a function of cell length is shown in Figure 3C.

To examine whether cell division was required for the specific subcellular localization of ParM, we treated the cells with cephalexin. This antibiotic inhibits FtsI and causes the cells to form filaments that are depleted of FtsZ ring structures (Pogliano *et al*., 1997). Figure 3A, k, shows a typical ParM–GFP-expressing cell after treatment with cephalexin. Fluorescent foci were seen spaced fairly evenly along the filament, and some of them appeared to be in the middle of the duplication process.

In cells that expressed the GFP–ParM fusion protein, specifically located foci were only observed in a minor fraction of the cells (10–20%) and the foci were less clear. When the GFP–ParM foci were visible, the subcellular localization was identical to that of the ParM–GFP fusion protein. Cells that expressed GFP itself or fusion proteins containing truncated ParM (Figure 2A) showed a uniform distribution of fluorescence (not shown). We also introduced the D170E mutation, which severely reduces the ATPase activity of ParM (Jensen and Gerdes, 1997), into the ParM–GFP fusion protein. ParM D170E–GFP did not localize (Figure 3A, l). Thus, ATPase activity seems to be required for localization of ParM.

Localization of ParM using IFM

To confirm that the localization of the ParM–GFP fusion protein observed here reflects the intracellular localization of the native ParM protein, we performed IFM using antibodies against ParM (Figure 3D). The ParM protein was expressed from a wild-type *parA* system present in the low copy number plasmid pRBJ460. IFM revealed a pattern of ParM localization that was clearly reminiscent of that observed using the ParM–GFP fusion protein (compare Figure 3D and A, a–j). Thus, it seems that ParM–GFP localizes to the same intracellular sites as native ParM, even though the GFP fusion protein is not fully functional.

Properties of ParR–GFP fusion proteins

We also constructed gene fusions between the second partitioning protein ParR and GFP (Figure 2B). The fusion to both the N- (ParR–GFP) and the C-terminus of GFP (GFP–ParR) exhibited biological activity (measured as repression of the *parA* promoter). Both types of fusion proteins showed a uniform distribution (Figure 3A, m). The presence of a *parA*-containing plasmid or expression of ParM did not lead to formation of specifically located fluorescent ParR–GFP foci (data not shown).

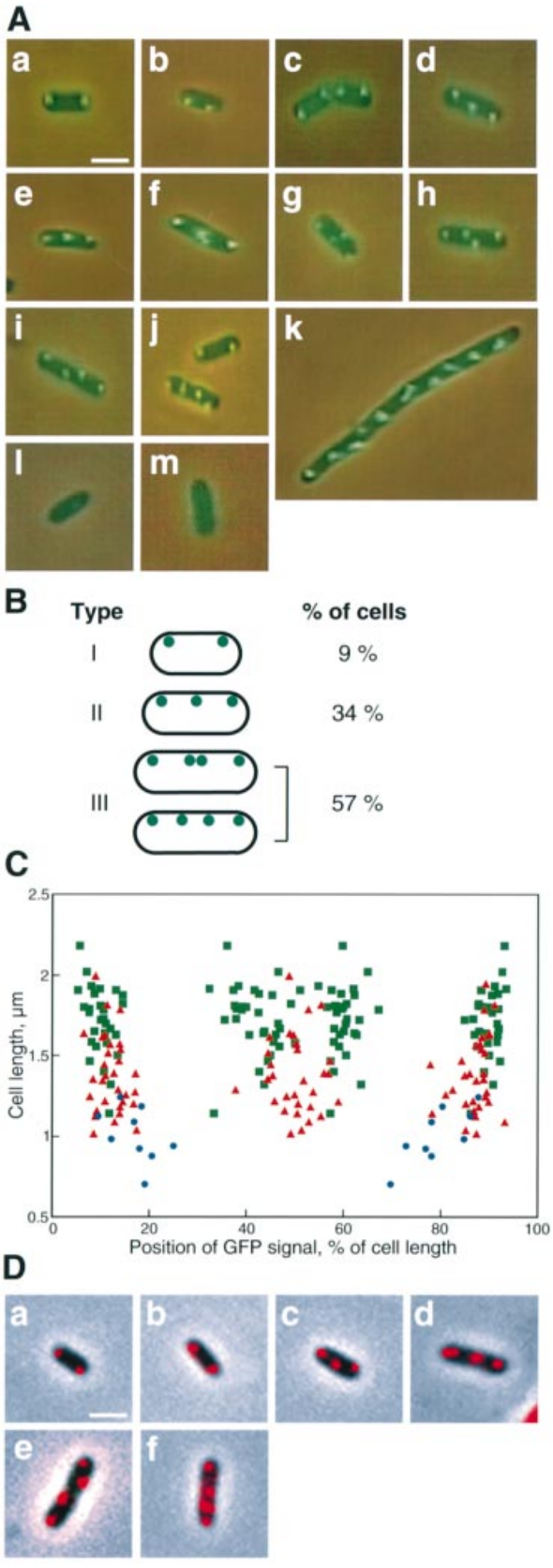

Fig. 3. Intracellular localization of ParM in *Escherichia coli* cells. (**A**) Combined phase-contrast and fluorescence microscopy images that illustrate the specific subcellular localization of ParM–GFP. The scale bar represents 1 µm. Three types of cells were observed: (a–c) cells with two foci located near the poles; (d–f) cells with three foci, where two foci were located near the poles and one was located at mid-cell; (h–j) cells with four foci, where two foci were located near the poles and two were located close to mid-cell. (k) Typical filamentous cell obtained by treating the cells with the antibiotic cephalexin. ParM–GFP formed fluorescent foci that were spaced fairly evenly along the filament. (l and m) Uniform distribution of GFP fluorescence in cells expressing ParM D170E–GFP or ParR–GFP, respectively. (**B**) Quantification of the three types of cells observed when ParM–GFP was expressed. (**C**) Measurements of the positions of the ParM–GFP foci from one cell pole as a function of cell length. Blue circles represent cells with two foci, red triangles represent cells with three foci, and green squares represent the four-foci cells. The strain used was KG22 carrying pRBJ420. (**D**) IFM localization of native ParM. Shown are overlays of the ParM IFM signals (red) and phase-contrast microscopy images. (a–b) Cells with two ParM foci; (c–d) three-foci cells; and (e–f) cells with four foci. The scale bar represents 1 µm. The strain used was MC1000 carrying pRBJ460.

Visualization of the subcellular localization of plasmids using the GFP–LacI assay

We then examined the intracellular localization of plasmids using the GFP–LacI system (Robinet *et al.*, 1996; Straight *et al.*, 1996). An array of repeated *lac* operators was inserted into a mini-F plasmid that contained either the *parA* system of R1 or no partitioning system. Thus, pRBJ460 is a mini-F plasmid that contains the *lacO* array and *parA*. Plasmid pRBJ461 is the corresponding *par*$^-$ control. The *lacO*-carrying plasmids were as stably maintained as plasmids that did not contain the *lacO* array (data not shown).

We expressed GFP–LacI from a second plasmid and subjected the cells to combined phase-contrast and fluorescence microscopy. Fluorescent dots that were localized to specific subcellular positions were observed in 85–95% of the cells (Figure 4A and B). The vast majority of the cells (all of the 711 examined) had one or two fluorescent foci. The size of the plasmids used here was ~28 kb, but since the plasmids most likely exist in a compact, supercoiled form *in vivo*, the positions of the fluorescent foci are expected to indicate the cellular localization of the replicons.

Figure 4A shows cells that contained the *parA* plasmid pRBJ460. In cells with one GFP focus only, the focus was located close to one of the cell poles (Figure 4A, a–c) or close to mid-cell (Figure 4A, d–f). In cells with two foci, the fluorescent dots most often were located towards both cell poles (Figure 4A, j–l) and less often close to each other at mid-cell (Figure 4A, g–i). The proportions of the different cell types are summarized in Figure 4C. Most importantly, the majority of the two-foci cells had symmetrically located foci, and asymmetrically located foci were rare (6% of the two-foci cells, type IV in Figure 4C).

We measured the positions of the GFP–LacI foci relative to the cell poles for cells of all types and all lengths. The polar GFP–LacI foci were found to be located at a fixed distance from the pole that coincides with the position of the polar ParM–GFP foci. The distributions of the GFP–LacI foci as a function of cell length are shown in Figure 4D. Whether the fluorescent foci in the one-dot cells were located towards the cell pole or towards mid-cell was independent of cell length. In a few of the two-dot cells, the foci were located symmetrically at positions in the cells where no foci were observed in the one-dot cells (e.g. the cell in Figure 4A, j, where the foci are located at 1/4 and 3/4 positions). They probably reflect intermediates in the DNA segregation process (i.e. replicons under migration towards the cell poles).

Figure 4B shows cells that contained the control plasmid without *parA*. In this case, localization was clearly less well defined (compare Figure 4D and E), and one-dot cells with a polar focus were more abundant (Figure 4C). The difference in plasmid localization for the two-dot cells was striking. Cells with asymmetrically located foci were abundant for the control plasmid (57% of the two-foci cells, type IV in Figure 4C). Thus, the presence of the *parA* system influenced the localization of the plasmid. The localization of the control plasmid, however, was not random. In this case, plasmid molecules were located mainly in the regions of the cells not occupied by the nucleoids. Random localization of *par*$^-$ plasmids to cytosol spaces but not the nucleoid spaces was also observed by Niki and Hiraga (1997).

Effect of cephalexin on the subcellular localization of plasmids

Figure 4A, m–o, shows typical localization patterns in cephalexin-treated filamentous cells containing the *parA*-carrying plasmid. In most cells, two to four foci were observed and, in the majority of the cells, the foci were located symmetrically. In the case of the control plasmid, the foci appeared to be located at random positions, and very few filaments contained symmetrically located foci (Figure 4B, j). These results confirm that the presence of the *parA* system influenced the intracellular localization of the plasmid and showed that lack of cell division and depletion of FtsZ ring structures did not abolish *parA*-mediated subcellular localization of the plasmid.

Co-localization of ParM and a parA-containing plasmid

Measurements of the intracellular positions of the ParM–GFP foci and the *parA* plasmid indicated that ParM and the plasmid co-localized. To show this directly, we simultaneously examined the intracellular localization of ParM using IFM (red signals in Figure 4F) and that of the *parA*-containing plasmid using GFP–LacI (green signals in Figure 4F). Overlays (i.e. combining the two signals from the same cell) of the red and green signals showed that the GFP–LacI foci fully or partially coincided with the ParM foci (the yellow colour in the overlay panels in Figure 4F shows coincidence of the ParM IFM and GFP–LacI fluorescence). Thus, within the resolution limits of light microscopy and the assays used here, the *parA*-containing plasmid appears to co-localize with the ParM partitioning protein.

Discussion

We examined the intracellular localization of the three components of the *parA* partitioning system of plasmid R1, i.e. ParM, ParR and *parC*-containing plasmids. We

Fig. 4. Intracellular localization of the *lacO* cassette containing plasmids in *E.coli* cells expressing the GFP–LacI fusion protein (A–E), and co-localization of GFP–LacI and ParM (F). In (A) and (D), the cells contained the *parA*-containing plasmid pRBJ460 and in (B) and (E) the cells contained the *par*$^-$ control plasmid pRBJ461. (**A** and **B**) Combined phase-contrast and fluorescence microscopy images that illustrate the different types of cells observed. The scale bar represents 1 μm. (A, a–c) and (B, a and b) Cells with one polar focus; (A, d–g) and (B, c and d) cells with one focus located close to mid-cell; (A, g–i) cells with two foci located close to mid-cell; (A, j–l) and (B, e) two-foci cells with foci located close to the poles; (B, f–i) cells with two foci that are located asymmetrically in the cell; (A, m–o) and (B, j) cephalexin-treated filamentous cells. (**C**) Quantification of the four different cell types observed. (**D** and **E**) Measurements of the positions of the GFP–LacI foci from one cell pole as a function of cell length. Purple diamonds represent cells with one fluorescent focus and blue circles represent two-foci cells. (**F**) Simultaneous IFM localization of ParM and localization of the *parA*-containing plasmid using the GFP–LacI assay. The first panel shows phase-contrast microscopy images, the second panel is the ParM IFM signal, the third panel is the GFP–LacI signal and the fourth panel is an overlay of the images. Yellow represents co-localization of the ParM IFM and the GFP–LacI signals. The scale bar represents 1 μm. The strain used was MC1000 carrying pRBJ460 or pRBJ461.

found that the ParM protein and *parA*-containing plasmids co-localize to specific sites close to the poles and close to mid-cell. This specific localization of the components strongly indicates that *parA* is a true partitioning system that stabilizes plasmids by securing ordered segregation of the plasmid molecules prior to cell division.

We observed a regular and dynamic localization pattern of ParM using both a ParM–GFP fusion protein and IFM

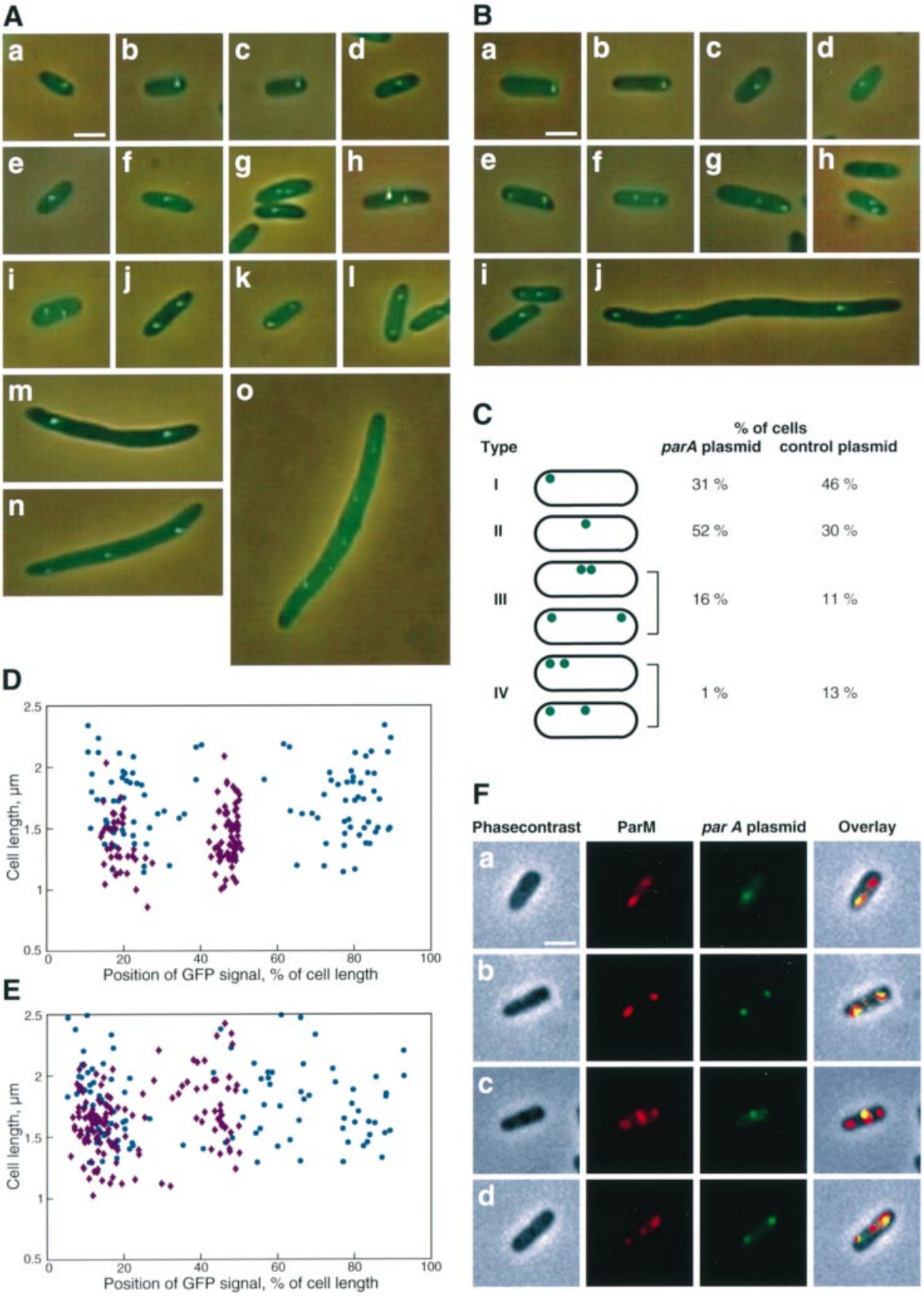

(Figure 3). Newborn cells contained two ParM foci close to but not at the cell poles. Upon cell growth, a new ParM focus appeared at mid-cell. Later in the cell cycle, the mid-cell focus duplicated. Concomitant with cell elongation, the two new foci at mid-cell migrated in opposite directions. Cell division between mid-cell foci then resulted in daughter cells with two polar foci. Localization is an intrinsic property of ParM, since ParM–GFP localized in the absence of other components of the *parA* system. Concomitant production of ParM or ParR from a second plasmid or the presence of a plasmid containing the *parA* system had no effect on the localization pattern of ParM–GFP or on the fraction of the cells that had clear foci (data not shown).

The ParM D170E–GFP mutant protein did not localize. We have shown previously that the D170E mutation reduces the ATPase activity of ParM and concomitantly abolishes its ability to support plasmid partitioning (Jensen and Gerdes, 1997). Thus, the ATPase activity of ParM is required both for partitioning and for its intracellular localization. This result is consistent with the inference that localization of ParM is essential for partitioning.

The intracellular localization of a *parA*-containing plasmid was examined using the GFP–LacI system. In cells that contained one GFP–LacI focus, the fluorescent focus was located either at mid-cell or close to one of the poles (Figure 4). In the cells that contained two fluorescent foci, the dots were located almost exclusively close to the poles. A few two-dot cells also had the foci at mid-cell. Most importantly, almost all of the two-foci cells exhibited a symmetrical pattern of localization (94%), whereas the control plasmid exhibited a more random distribution (compare Figure 4D and E). In a few of the two-foci cells, the plasmids were located at intermediate positions where no ParM–GFP foci were observed (Figure 4A, j). Since the foci in these cells were located symmetrically, they may reflect plasmids migrating to the cell poles. The low abundance of such intermediates is consistent with rapid plasmid movement towards the cell poles (discussed further below).

Comparison of the positions of the ParM–GFP and GFP–LacI foci indicates that the *parA*-containing plasmid co-localizes with ParM–GFP (close to the poles or close to mid-cell; compare Figures 3C and 4D). The co-localization was shown directly by simultaneous visualization of ParM using IFM and of the *parA*-containing plasmid using the GFP–LacI assay in the same cells. As seen in Figure 4F, overlay of the fluorescent signals clearly demonstrates co-localization. Generally, more ParM foci than plasmid foci were observed (e.g. the cells in Figure 4F, c, have one plasmid and three ParM foci). The function of additional ParM foci could be to prepare for plasmid segregation in the succeeding cell cycle.

It is reasonable to suggest that ParM aggregates close to the cell poles and mid-cell via the interaction with a host-encoded factor. Experiments with cephalexin showed that the localization of ParM and of the *parA*-carrying plasmid was unaffected by inhibition of cell division and depletion of FtsZ ring structures. Therefore, FtsZ ring structures are probably not involved in the localization process.

Our data are consistent with the proposal that the polarly located ParM protein tethers the plasmids to the polar regions until septum formation has been completed. We have shown previously that ParM interacts with ParR bound to *parC* (Jensen *et al*., 1998). Tethering of the *parA*-containing plasmid to the polar ParM foci could be achieved if ParR bound to *parC* interacts with ParM.

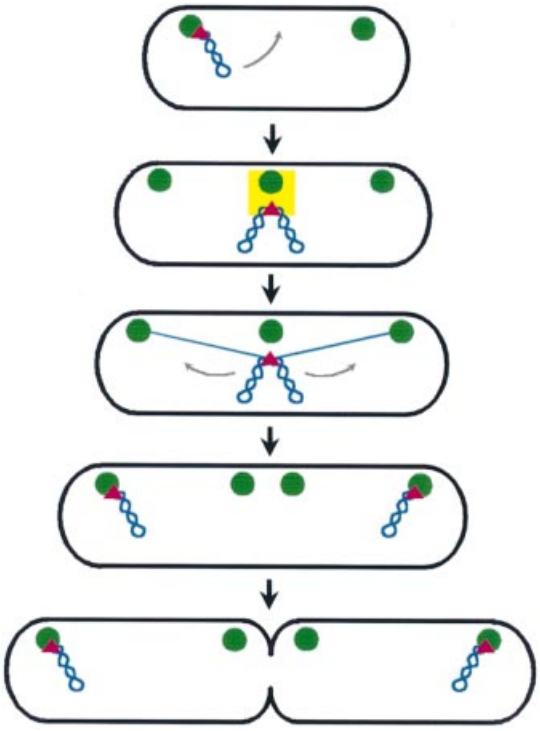

Fig. 5. Model for *parA*-mediated plasmid partitioning during the cell cycle. Green circles represent ParM foci and red triangles ParR bound to the *parC* centromere in a supercoiled plasmid (blue). A yellow square represents the DNA replication apparatus that, according to Lemon and Grossman (1998), is anchored at mid-cell, and lines represent an apparatus that may be responsible for translocation of plasmid molecules from mid-cell to the cell pole. Immediately after cell division, a plasmid is tethered to one of the poles via ParM. The DNA replication machinery moves the plasmid to mid-cell where it is replicated. Rapidly after replication, ParR pairs the newly replicated plasmids. The plasmids are released and moved rapidly to the cell poles. According to this model, ParM at mid-cell becomes polar in the next cell division cycle.

A simple model that explains plasmid partitioning

Recently, we demonstrated that ParR mediates specific pairing *in vitro* of *parC*-containing DNA molecules (Jensen *et al*., 1998). We believe that the symmetric distribution of the intermediate foci in cells with two GFP–LacI foci (Figure 4D) is consistent with the suggestion that *parA* mediates plasmid pairing at mid-cell. The observed co-localization of plasmids and the ParM protein further indicates that ParM tethers *parA*-containing plasmids close to the cell poles. These results support a simple model in which plasmid pairing at mid-cell is followed by active movement to the cell poles. Plasmid pairing at mid-cell is also consistent with the recent finding that the DNA replication machinery is present at mid-cell (Lemon and Grossman, 1998). This suggests that the plasmids move from the cell pole to mid-cell as part of their replication cycle. After replication at mid-cell, the twin daughter DNA molecules are paired at *parC*. Subsequently, the paired molecules are moved to the cell poles by the

Table I. Plasmids used and constructed

Plasmid	Relevant genotypes	Replicon	Resistance	Reference
pEGFP	P_{lac}::*gfp F64L S65T* (mut1)	pUC	Amp	Clontech
pSG20	P_{ara}::*gfp-lacI araC*	pUC	Amp	Gordon *et al.* (1997)
pAFS59	*lacO* cassette	pUC	Amp	Straight *et al.* (1996)
pFA10	*sop*$^-$ *parA*	mini-F	Kan	Gerdes and Molin (1986)
pFB10	*sop*$^-$ *hok/sok*	mini-F	Kan	K.Gerdes (unpublished)
pDD19	*parA*	pUC	Amp	Dam and Gerdes (1994)
pDD1509K	*parC* Δ*parM parR*	mini-R1	Kan	Jensen *et al.* (1994)
pAB1503	*parA*	mini-R1	Kan	Breüner *et al.* (1996)
pRBJ338	*parC parM D170E parR*	mini-R1	Amp	Jensen and Gerdes (1997)
pRBJ430	P_{lac}::*parM-gfp*	pUC	Amp	this work
pRBJ431	P_{lac}::*parR-gfp*	pUC	Amp	this work
pRBJ432	P_{lac}::*gfp-parM*	pUC	Amp	this work
pRBJ433	P_{lac}::*gfp-parR*	pUC	Amp	this work
pRBJ451	P_{lac}::*parM*Δ*N30-gfp*	pUC	Amp	this work
pRBJ452	P_{lac}::*parM*Δ*N60-gfp*	pUC	Amp	this work
pRBJ453	P_{lac}::*parM*Δ*C30-gfp*	pUC	Amp	this work
pRBJ454	P_{lac}::*parM*Δ*C60-gfp*	pUC	Amp	this work
pRBJ455	P_{lac}::*parM D170E-gfp*	pUC	Amp	this work
pRBJ460	*sop*$^-$ *parA lacO* cassette	mini-F	Kan	this work
pRBJ461	*sop*$^-$ *hok/sok lacO* cassette	mini-F	Kan	this work

partitioning apparatus. The model is shown schematically in Figure 5. The active plasmid movement probably requires host cell components in co-operation with the plasmid-encoded factors. Tethering of the plasmids close to the cell poles keeps them in their proper positions until the septum has formed at mid-cell.

The intracellular localization of the components of other partitioning systems has also been studied. The P1 and F plasmids localize either at mid-cell or at the 1/4 and 3/4 positions in the cell (Gordon *et al.*, 1997; Niki and Hiraga, 1997). The subcellular localization of SopB–GFP is consistent with the positioning of F in the cell cycle (Kim and Wang, 1998). Directional movement of newly replicated plasmid molecules at mid-cell to the cell quarter sites may be responsible for plasmid stabilization by the *sop* and *par* system. However, the localization of the *parA*-containing plasmid is clearly different from that of the P1 and F plasmids. That the difference is real is supported by the observation that an R1 *parA*-containing plasmid was segregated efficiently into *E. coli* minicells, whereas plasmids carrying P1 *par* or F *sop* were not (Eliasson *et al.*, 1992).

The chromosomal partitioning proteins Spo0J of *B.subtilis* and ParA and ParB of *C.crescentus* are associated with regions of the nucleoids that usually are located close to the cell poles. In some cells with two separated nucleoids, Spo0J foci near mid-cell were also observed. The foci were found to replicate and migrate rapidly within the cell (Glaser *et al.*, 1997; Lin *et al.*, 1997; Mohl and Gober, 1997; Sharpe and Errington, 1998; Teleman *et al.*, 1998). The Spo0J protein binds to at least eight sites in the origin-proximal region of the chromosome (Lin and Grossman, 1998). As expected from this, the origin-proximal region of the *B.subtilis* chromosome localized to the same positions as Spo0J and migrated with a similar pattern. This indicates that Spo0J is involved in tethering the origin-proximal part of the *B.subtilis* chromosome to positions near the poles (Lewis and Errington, 1997; Webb *et al.*, 1997, 1998; Teleman *et al.*, 1998). The origin-proximal region of the *E.coli* chromosome was found to localize and migrate with a pattern similar to that of the *B.subtilis* chromosome (Gordon *et al.*, 1997; Niki and Hiraga, 1998). Interestingly, the distribution pattern of the ParM foci and the *parA*-carrying plasmid observed here was similar to that of the *B.subtilis* Spo0J protein and the origin-proximal regions of the *B.subtilis* and *E.coli* chromosomes. This suggests that *parA* may specify a partitioning mechanism that is perhaps related to that of the bacterial chromosomes.

Materials and methods

Bacterial strains and plasmids

The *E.coli* K-12 strain KG22 (C600 *lacI*^{q} *lacZ*Δ*M15 r*$^-$ *m*$^+$; obtained from the Mogens Trier strain collection) was used as host strain in all experiments involving ParM, ParR and GFP fusions. The strain STBL2 [F$^-$ *mcrA*Δ (*mcrBC-hsdRMS-mrr*) *recA1 endA1 lon gyrA96 thi-1 supE44 relA1*$^-$ λ$^-$ Δ (*lac-proAB*); Gibco-BRL] was used for construction of plasmids containing the array of *lacO* sites. The strain MC1000 [*araD139*Δ (ara, leu)7697 Δ*lac X74 galU galK strA*; Casadaban and Cohen (1980)] was used as host in all experiments involving GFP–LacI fusions. All plasmids used and constructed are listed in Table I.

Construction of plasmids

To construct fusions between *parM*, *parR* and *gfp*, the following oligonucleotides were used in PCRs as described below:

ParA202B, 5′-CCCGGATCCCATGTTGGTATTCATTGATGA-3′;
ParA202C, 5′-GGACGAGCTGTACAAGGCAGCTATGTTGGTATTCA-TTGATGA-3′;
ParA290, 5′-CCCGGATCCCAGCTTCAAACGCGAGTGG-3′;
ParA380, 5′-CCCGGATCCCAGCCCGGATGCTGTAGTC-3′;
ParA939, 5′-CGCGGCCATGGCAAGTTTACGAAGTGCTTCATT-3′;
ParA1029, 5′-CGCGGCCATGGCTGCATCGCATATTAATTCTGC-3′;
ParA1122, 5′-CGCGGCCATGGCATTACCTATGAGATACATAC-3′;
ParA1124, 5′-CCCGAATTCTTAATTACCTATGAGATACAT-3′;
ParA1165B, 5′-CCCGGATCCCATGGACAAGCGCAGAACC-3′;
ParA1165C, 5′-GGACGAGCTGTACAAGGCAGCTATGGACAAGCGCA-GAACC-3′;
ParA1476, 5′-CGCGGCCATGGCATTTATTAGCTTCATCGCAT-3′;
ParA1478, 5′-CCCGAATTCTTAATTTATTAGCTTCATCGC-3′.

The *parM* or *parR* fusions to the N-terminus of *gfp*, which are listed in Table I, were generated by PCR using the following pairs of oligonucleotides as primers: pRBJ430, ParA202B and ParA1122; pRBJ431, ParA1165B and ParA1476; pRBJ451, ParA290 and ParA1122; pRBJ452, ParA280 and ParA1122; pRBJ453, ParA202B and ParA1029; pRBJ454, ParA202B and ParA939; and pRBJ455, ParA202B and ParA1122. The PCR fragments were digested with *Bam*HI and *Nco*I and

inserted into pEGFP. The *parM* or *parR* fusions to the C-terminus of *gfp* were generated using the following pairs of oligonucleotides as primers: pRBJ432, ParA202C and ParA1124; and pRBJ433, ParA1165C and ParA1478. The PCR fragments were digested with *Bsr*GI and *Eco*RI and inserted into pEGFP. The *parA*-containing plasmid pDD19 was used as template in all PCRs, except for the construction of pRBJ455 where pRBJ338 was used instead.

To construct mini-F plasmids containing the *lacO* cassette, the 10 kbp *Sal*I–*Xho*I fragment of plasmid pAFS59 was inserted into the unique *Sal*I sites of the 18 kbp plasmids pFA10 and pFB10, resulting in the plasmids pRBJ460 and pRBJ461, respectively. Plasmid pRBJ460 is a *sop*$^-$ mini-F plasmid that contains the *parA* system and the *lacO* cassette. The control plasmid pRBJ461 is a *sop*$^-$ mini-F plasmid that contains the *hok/sok* post-segregational killer system and the *lacO* cassette. The plasmids pRBJ460 and pRBJ461 are stably maintained due to *parA* and *hok*/*sok* of R1, respectively. The *hok*/*sok* system stabilizes plasmids by post-segregational killing and therefore does not influence the subcellular localization of the plasmid.

Growth conditions and media

To express the ParM, ParR and GFP fusion proteins, strain KG22 containing the relevant plasmid was grown for at least eight generations in A + B minimal medium (Clark and Maaloe, 1967) supplemented with 0.2% glucose, 1 μg/ml thiamine, 50 μg/ml casamino acids and 100 μg/ml ampicillin at 30°C. Expression of the fusion proteins was induced by adding 50–100 μM IPTG to the medium. Induction for 3–4 h before microscopy yielded the best results. Under these growth conditions, the generation time of the strain was ~70 min. Growth at higher temperatures, in rich medium or expression of higher amounts of fusion protein resulted in non-specific aggregation of ParM–GFP.

To express the GFP–LacI fusion protein, strain MC1000 containing the GFP–LacI expression plasmid pSG20 and the relevant mini-F test plasmid was grown for at least eight generations in LB medium (Bertani, 1951) supplemented with 100 μg/ml ampicillin and 50 μg/ml kanamycin at 20°C. Expression of GFP–LacI was induced by adding 0.2% L-arabinose to the media. After 15–30 min, 0.2% glucose was added to repress the synthesis of GFP–LacI, and growth was continued for 2–3 h before microscopy. The generation time of the strain was ~2 h under these growth conditions. A short induction of GFP–LacI synthesis followed by several hours of growth gave the brightest signals, probably because it allowed additional GFP to mature. Under these growth and induction conditions, no fluorescent dots were observed in strains that did not contain the *lacO* cassette, showing that GFP–LacI did not form non-specific aggregates. Growth at higher temperatures or when more GFP–LacI was expressed resulted in non-specific aggregation of GFP–LacI. When relevant, 10 μg/ml cephalexin was added to the growth medium and the cells were allowed to form filaments for 2–3 h before microscopy.

Microscopy

GFP-expressing cells were examined either immediately (living cells) or after chemical fixation. To fix the cells, formaldehyde (to 2%) and glutaraldehyde (to 0.1%) were added directly to a sample of the culture. The cells were incubated at room temperature for 15 min and at 0°C for 30 min, collected by centrifugation and resuspended in 0.9% saline. Living cells were immobilized on microscope slides using a thin film of agarose as described by Glaser *et al.* (1997) and fixed cells were immobilized using poly-L-lysine-treated slides or SuperFrost Plus slides (Menzel Gläser). The cells were observed with a Leica DMRBE fluorescence and phase-contrast microscope with a Leica PL APO 100×/1.40 objective. Pictures were obtained with a colour CCD camera connected to a computer. The GFP foci locations were measured using Scion Image 1.62a (Scion Corporation). For all measurements and statistical analysis of GFP foci positions, at least 200 cells from randomly selected fields were analysed.

The described localization pattern of ParM–GFP was observed both in living and in fixed cells. In living cells, the ParM–GFP fluorescent foci were visible only for a short period after mounting the cells on the slide. Mounting the cells on a thin layer of agarose gave more stable fluorescent foci than when the cells were adsorbed to poly-L-lysine-treated slides. The dissipation of the ParM–GFP signals in unfixed cells could be caused by cell death after mounting. Mild chemical fixation made the GFP signal more stable and allowed us to store the cells for weeks without loss of the specifically located fluorescent signals. However, living cells were used in most of the work.

Immunofluorescence microscopy

Cells were grown and induced as described for cells expressing the GFP–LacI protein. The cells were fixed using methanol as described by Teleman *et al.* (1998) and IFM was performed as described by Addinall *et al.* (1996). Affinity-purified rabbit anti-ParM antibodies were used at a 1:20 dilution, and rhodamine-conjugated goat anti-rabbit IgG antibodies (Jackson ImmunoResearch) were used at a 1:200 dilution. IFM-stained cells were observed with a Nikon Eclipse E800 fluorescence and phase-contrast microscope with a Nikon Plan Apo 100×/1.40 objective. Pictures were obtained with a cooled CCD camera connected to a computer. The images were acquired and processed using Metamorph 3.6A (Universal Imaging Corp.).

Cells that did not express ParM had no detectable IFM signals, and fixation using formaldehyde and glutaraldehyde as described by Addinall *et al.* (1996) gave ParM localization to the same intracellular sites.

Acknowledgements

We thank Pia Hovendal for excellent technical assistance, Dr Issinger and Dr Shapiro for use of their microscopes, Rob Wheeler for help with IFM, and Hansjörg Lehnherr and members of the Lucy Shapiro laboratory for critical reading of the manuscript. This work was supported by the Danish Biotechnology Program (CIS-FEM), the Carlsberg Foundation and the Plasmid Foundation.

References

Abeles,A.L., Friedman,S.A. and Austin,S.J. (1985) Partition of unit-copy miniplasmids to daughter cells. III. The DNA sequence and functional organization of the P1 partition region. *J. Mol. Biol.*, **85**, 261–272.

Addinall,S.G., Bi,E. and Lutkenhaus,J. (1996) FtsZ ring formation in *fts* mutants. *J. Bacteriol.*, **178**, 3877–3884.

Bertani,G. (1951) Studies on lysogenesis. I. The mode of phage liberation by lysogenic *Escherichia coli*. *J. Bacteriol.*, **62**, 293–300.

Breüner,A., Jensen,R.B., Dam,M., Pedersen,S. and Gerdes,K. (1996) The centromere-like *parC* locus of plasmid R1. *Mol. Microbiol.*, **20**, 581–592.

Casadaban,M.J. and Cohen,S.N. (1980) Analysis of gene control signals by DNA fusion and cloning in *Escherichia coli*. *J. Mol. Biol.*, **138**, 179–207.

Clark,D.J. and Maaloe,O. (1967) DNA replication and the division cycle in *Escherichia coli*. *J. Mol. Biol.*, **23**, 99–112.

Cormack,B.P., Valdivia,R.H. and Falkow,S. (1996) FACS-optimized mutants of the green fluorescent protein (GFP). *Gene*, **173**, 33–38.

Dam,M. and Gerdes,K. (1994) Partitioning of plasmid R1. Ten direct repeats flanking the *parA* promoter constitute a centromere-like partition site *parC*, that expresses incompatibility. *J. Mol. Biol.*, **236**, 1289–1298.

Davis,M.A. and Austin,S.J. (1988) Recognition of the P1 plasmid centromere analog involves binding of the ParB protein and is modified by a specific host factor. *EMBO J.*, **7**, 1881–1888.

Davis,M.A., Martin,K.A. and Austin,S.J. (1992) Biochemical activities of the ParA partition protein of the P1 plasmid. *Mol. Microbiol.*, **6**, 1141–1147.

Eliasson,Å., Bernander,R., Dasgupta,S. and Nordström,K. (1992) Direct visualization of plasmid DNA in bacterial cells. *Mol. Microbiol.*, **6**, 165–170.

Gerdes,K. and Molin,S. (1986) Partitioning of plasmid R1. Structural and functional analysis of the *parA* locus. *J. Mol. Biol.*, **190**, 269–279.

Gerdes,K., Gultyaev,A.P., Franch,T., Pedersen,K. and Mikkelsen,N.D. (1997) Antisense RNA-regulated programmed cell death. *Annu. Rev. Genet.*, **31**, 1–31.

Glaser,P., Sharpe,M.E., Raether,B., Perego,M., Ohlsen,K. and Errington,J. (1997) Dynamic, mitotic-like behavior of a bacterial protein required for accurate chromosome partitioning. *Genes Dev.*, **11**, 1160–1168.

Gordon,G.G., Sitnikov,D., Webb,C.D., Teleman,A., Straight,A., Losick,R., Murray,A.W. and Wright,A. (1997) Chromosome and low copy plasmid segregation in *E.coli*: visual evidence for distinct mechanisms. *Cell*, **90**, 1113–1121.

Harry,E.J. (1997) Illuminating the force: bacterial mitosis? *Trends Microbiol.*, **5**, 295–297.

Hiraga,S. (1992) Chromosome and plasmid partition in *Escherichia coli*. *Annu. Rev. Biochem.*, **61**, 283–306.

Ireton,K., Gunther,N.W.,IV and Grossman,A.D. (1994) *spo0J* is required for normal chromosome segregation as well as initiation of sporulation in *Bacillus subtilis*. *J. Bacteriol.*, **176**, 5320–5329.

Jensen,R.B. and Gerdes,K. (1995) Programmed cell death in bacteria: proteic plasmid stabilization systems. *Mol. Microbiol.*, **17**, 205–210.

Jensen,R.B. and Gerdes,K. (1997) Partitioning of plasmid R1. The ParM protein exhibits ATPase activity and interacts with the centromere-like ParR–*parC* complex. *J. Mol. Biol.*, **269**, 505–513.

Jensen,R.B., Dam,M. and Gerdes,K. (1994) Partitioning of plasmid R1. The *parA* operon is autoregulated by ParR and its transcription is highly stimulated by a downstream activating element. *J. Mol. Biol.*, **236**, 1299–1309.

Jensen,R.B., Lurz,R. and Gerdes,K. (1998) Mechanism of DNA segregation in prokaryotes: replicon pairing by *parC* of plasmid R1. *Proc. Natl Acad. Sci. USA*, **95**, 8550–8555.

Kim,S.-K. and Wang,J.C. (1998) Localization of F plasmid SopB protein to positions near the poles of *Escherichia coli* cells. *Proc. Natl Acad. Sci. USA*, **95**, 1523–1527.

Lemon,K.P. and Grossman,A.D. (1998) Localization of bacterial DNA polymerase: evidence for a factory model of replication. *Science*, **282**, 1516–1519.

Lewis,P.J. and Errington,J. (1997) Direct evidence for active segregation of *oriC* regions of the *Bacillus subtilis* chromosome and co-localization with the Spo0J partitioning protein. *Mol. Microbiol.*, **25**, 945–954.

Lin,D.C. and Grossman,A.D. (1998) Identification and characterization of a bacterial chromosome partitioning site. *Cell*, **92**, 675–685.

Lin,D.C., Levin,P.A. and Grossman,A.D. (1997) Bipolar localization of a chromosome partition protein in *Bacillus subtilis*. *Proc. Natl Acad. Sci. USA*, **94**, 4721–4726.

Mohl,D.A. and Gober,J.W. (1997) Cell cycle-dependent polar localization of chromosome partitioning proteins in *Caulobacter crescentus*. *Cell*, **88**, 675–684.

Mori,H., Mori,Y., Ichinose,C., Niki,H., Ogura,T., Kato,A. and Hiraga,S. (1989) Purification and characterization of SopA and SopB proteins essential for F plasmid partitioning. *J. Biol. Chem.*, **264**, 15535–15541.

Niki,H. and Hiraga,S. (1997) Subcellular distribution of actively partitioning F plasmid during the cell division cycle in *E.coli*. *Cell*, **90**, 951–957

Niki,H. and Hiraga,S. (1998) Polar localization of the replication origin and terminus in *Escherichia coli* nucleoids during chromosome partitioning. *Genes Dev.*, **12**, 1036–1045.

Nordström,K. and Austin,S. (1989). Mechanisms that contribute to the stable segregation of plasmids. *Annu. Rev. Genet.*, **23**, 37–69.

Ogura,T. and Hiraga,S. (1983) Mini-F plasmid genes that couple host cell division to plasmid proliferation. *Cell*, **32**, 351–360.

Pogliano,J., Pogliano,K., Weiss,D.S., Losick,R. and Beckwith,J. (1997) Inactivation of FtsI inhibits constriction of the FtsZ cytokinetic ring and delays the assembly of FtsZ rings at potential division sites. *Proc. Natl Acad. Sci. USA*, **94**, 559–564.

Robinett,C., Straight,A., Li,G., Willhelm,C., Sudlow,G., Murray,A. and Belmont,A. (1996) *In vivo* localization of DNA sequences and visualization of large-scale chromatin organization using lac operator/repressor recognition. *J. Cell Biol.*, **135**, 1685–1700.

Sharpe,M.E. and Errington,J. (1996) The *Bacillus subtilis soj–spo0J* locus is required for a centromere-like function involved in prespore chromosome partitioning. *Mol. Microbiol.*, **21**, 501–509.

Sharpe,M.E. and Errington,J. (1998) A fixed distance for separation of newly replicated copies of *oriC* in *Bacillus subtilis*: implications for co-ordination of chromosome segregation and cell division. *Mol. Microbiol.*, **28**, 981–990.

Sharpe,M.E. and Errington,J. (1999) Upheaval in the bacterial nucleoid an active chromosome segregation mechanism. *Trends Genet.*, **15**, 70–74.

Straight,A.F., Belmont,A.S., Robinett,C.C. and Murray,A.W. (1996) GFP tagging of budding yeast chromosomes reveal that protein–protein interactions can mediate sister chromatid cohesion. *Curr. Biol.*, **6**, 1598–1608.

Teleman,A.A., Graumann,P.L., Lin,D.C., Grossman,A.D. and Losick,R. (1998) Chromosome arrangement within a bacterium. *Curr. Biol.*, **8**, 1102–1109.

Watanabe,E., Wachi,M., Yamasaki,M. and Nagai,K. (1992) ATPase activity of SopA, a protein essential for active partitioning of F plasmid. *Mol. Gen. Genet.*, **234**, 346–352.

Webb,C.D., Teleman,A., Gordon,S., Straight,A., Belmont,A., Lin,D.C., Grossman,A.D., Wright,A. and Losick,R. (1997) Bipolar localization of the replication origin regions of the chromosomes in vegetative and sporulating cells of *B.subtilis*. *Cell*, **88**, 667–674.

Webb,C.D., Graumann,P.L., Kahana,J.A., Teleman,A.A., Silver,P.A. and Losick,R. (1998) Use of time-lapse microscopy to visualize rapid movement of the replication origin region of the chromosome during the cell cycle in *Bacillus subtilis*. *Mol. Microbiol.*, **28**, 883–892.

Wheeler,R.T. and Shapiro,L. (1997) Bacterial chromosome segregation: is there a mitotic apparatus? *Cell*, **88**, 577–579.

Received December 11, 1998; revised and accepted May 21, 1999